RSC Advances

PAPER

View Article Online
View Journal | View Issue

Cite this: *RSC Adv.*, 2024, **14**, 31461

Direct ink writing of high explosive composites containing metal–organic frameworks†

Eun-Young Kim,[ab] Seong han Kim,[c] Mingu Han*[c] and Su-Young Moon *[a]

Smart weapon systems are being miniaturised for widespread application in high-energy materials, necessitating the development of processable and printable high explosive (HEs) composites that can be detonated with a small critical diameter. This study presents an efficient strategy for fabricating HE composites with exceptional detonation performance. We developed an HE ink based on 1,3,5-trinitro-1,3,5-triazinane (RDX), consisting of a glycidyl azide polymer (GAP) as a binder and a metal–organic framework (MOF) as an additive. This ink was deposited on an aluminium plate using direct ink writing (DIW). The resulting RDX/MOF composite demonstrated a significantly lower critical diameter (~720 μm) for detonation compared to a composite without the MOF. This reduction in critical diameter is attributed to the pores inside the MOFs, which enhanced the transfer of heat during detonation, creating an artificial hot-spot that sustained continuous explosion. The fabricated RDX/MOF composite offers a promising approach for developing miniaturized smart weapon systems with improved detonation characteristics.

Received 2nd May 2024
Accepted 11th September 2024

DOI: 10.1039/d4ra03241a

rsc.li/rsc-advances

Introduction

As interest in miniaturizing and integrating complex weapon systems grows,[1–3] there is a pressing demand to advance technology in line with the trend of reducing the size of various sophisticated components and functionalities into unified systems.[4] This could involve shrinking the size of existing devices, such as missiles, drones, and surveillance equipment to create more efficient and versatile weapons that can be seamlessly integrated into military operations. High explosives, as key components of weapon systems, need to be meticulously incorporated into these systems. Commercial high explosives (Fig. 1a), such as RDX, HMX, CL-20, and TNT,[5–7] predominantly exist in granular or powdery forms. For effective application, they must be transformed into a solution-processable phase. Numerous studies have focused on developing high explosive (HE) inks for printing and patterning purposes.[8–11]

HE inks generally consist of explosives, binders, solvents, and additives (Fig. 1).[12–14] The binder serves as the matrix that holds the explosive particles together in a cohesive mixture[15–17] and ensures proper adhesion to the substrate during printing and patterning processes. Furthermore, the binder influences the overall stability, compatibility, and performance of the printed explosive materials, making its selection crucial for optimising the properties and functionality of HE inks for various applications. Energetic polymers containing high-energy functional groups such as nitro, nitramino, difluoroamino, and azido groups are used for patterning powdered explosives. The properties of the polymer binder used to enclose high-energy-material-based ink on the substrate significantly impact the detonation performance of the composite. Notable binders include 3-nitratomethyl-3-methyl oxetane (NIMBO)[18,19] glycidyl nitrate (GLYN)[20,21] and glycidyl azide polymer (GAP).[22,23] These polymers typically have low glass-transition temperatures (Fig. 1b). Among them, GAP is considered an effective binder with a high energy potential compared to other energetic polymers due to its azido group ($-N_3$), which increases the detonation effect by releasing a significant amount of nitrogen gas during detonation.

Additives in HE ink are substances incorporated into the formulation to modify or enhance specific properties of the ink or the final printed explosive material (Fig. 1c). Depending on the specific requirements of the printing process and the desired characteristics of the end product, these additives can serve various purposes. Al powder is a common additive found in HE inks; it is widely used in research on additives for high explosives.[24–27] When combined with explosives, it improves explosion performance by increasing the explosion heat and bubble energy. Other additives include emulsifiers, such as Viton A, and PVA that are used in CL-20 based ink to stabilize the interface between components, reducing defects and critical detonation size.[28]

For the main constituent of HE inks, the explosives, RDX and HMX, composed of nitroamine groups, have been traditionally employed in weaponry due to their high energy density and

[a]*Hydrogen & C1 Gas Research Center, Chemical & Process Technology, Korea Research Institute of Chemical Technology, Daejeon 34114, South Korea. E-mail: msy1609@krict.re.kr*

[b]*Department of Chemical and Biomolecular Engineering, Yonsei University, 50 Yonsei-ro, South Korea*

[c]*4th R&D Institute 2nd Directorate Agency for Defense Development, Yuseong, P O Box 35-42, Daejeon 34186, South Korea. E-mail: mingu@addf.re.kr*

† Electronic supplementary information (ESI) available. See DOI: https://doi.org/10.1039/d4ra03241a

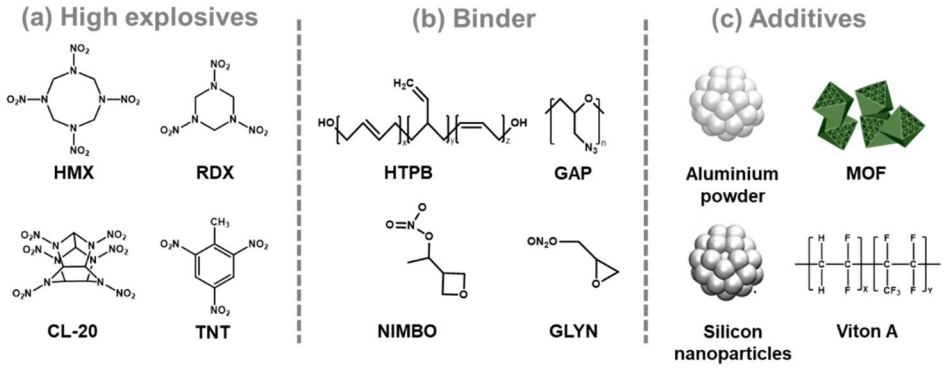

Fig. 1 Representative structures of (a) high energy materials and (b) polymer binder and (c) images of additives.

straightforward synthesis. To enhance their safety and customize their properties for specific applications, they are often combined with polymers or waxes to form polymer-bonded explosives (PBX). Although PBXs mitigate sensitivity concerns, their detonation performance is limited at small charge sizes, restricting their application in the miniaturization and integration of complex weapon systems.

We hypothesised that porous nanoparticles with uniform nanopores and high pore volumes, such as metal–organic frameworks (MOFs), in combination with high explosives could promote active detonation by providing artificial hot spots. In this study, RDX-MOF inks made of RDX-based inks containing highly porous materials and MOFs were prepared to enhance detonation performance and patterned using direct ink writing (DIW). The resulting patterned RDX-MOF composites demonstrated enhanced detonation performance, detonating at a lower critical diameter (720 μm) compared to RDX ink.

Experimental

Materials

Chromium(III) nitrate nonahydrate ($Cr(NO_3)_3 \cdot 9H_2O$, 99%), hydrofluoric acid (HF, 48 wt% in H_2O, ≥99.99% trace metal basis), 1,4-butanediol (BDO, 99%), sodium azide (99%), sodium sulfate (99%, anhydrous, powder), BF_3-dimethyletherate (98%), epichlorohydrin (ECH, 99%) and methylene chloride (99.8%) were obtained from Sigma-Aldrich. *N*,*N*-Dimethylformamide (DMF, 99.5% purity), and ethyl alcohol (99% purity) were purchased from Samchun, Korea. Terephthalic acid (H_2BDC) was supplied by Tokyo Chemical Industry (TCI). 1,3,5-Trinitro-1,3,5-triazinane (RDX) was provided by the Agency for Defense Development (ADD). All reagents were used as received, without further purification.

Synthesis of MIL-101(Cr)

$Cr(NO_3)_3 \cdot 9H_2O$ (1.68 mmol, 400 mg) and H_2BDC (1 mmol, 166 mg) were dissolved in a mixture of HF and H_2O (0.02 mL/4.8 mL). After mixing, the solution was heated at 220 °C for 18 h in a hydrothermal reactor. After cooling to 25 °C, a green precipitate was isolated from the unreacted chemicals by centrifuge and washed several times with DMF, H_2O, and ethanol. The resulting product was dried at 150 °C for 24 h under vacuum. Next the as-synthesised MIL-101(Cr) was immersed in 100 mL of 0.03 M aqueous NH_4F solution at 60 °C for 12 h for activation. Finally, a green precipitate was obtained after purification with H_2O and dried at 150 °C for 24 h under vacuum.

Synthesis of glycidyl azide polymer

Glycidyl azide polymer (GAP) was synthesised in two steps: synthesis of polyepichlorohydrin (PECH) and conversion of PECH to GAP (Fig. S2†).

1.33 g (14.4 mmol) of 1,4-butanediol (BDO) dissolved in methylene chloride (75 mL) was placed in a flask under a nitrogen purge. BF_3-dimethyletherate was added to the solution and stirred at room temperature for 1 h. After cooling the reaction vessel to 0 °C, 46.66 g (504.4 mmol) of ECH was injected dropwise at a rate of 0.1 mL min^{-1} for 12 h. The reaction was allowed to continue for another 12 h at room temperature and then quenched by adding water. The organic phase containing PECH was extracted with methylene chloride and washed several times with distilled water. Then, it was dried over sodium sulfate and filtered. Finally, the solvent was evaporated at 40 °C using a rotary evaporator and dried at 60 °C in a vacuum oven. A yellow liquid with high viscosity was obtained.

PECH (28 g) was dissolved in *N*,*N*-dimethylformamide (DMF; 100 mL). The solution was heated to 120 °C under a nitrogen atmosphere and 25 g of sodium azide was added to the mixture. After 12 h, the reaction was quenched by adding water and filtered to remove the unreacted reagents. The organic phase containing GAP was extracted with methylene chloride and washed several times with distilled water. Then, it was dried over sodium sulfate and filtered. Finally, the solvent was evaporated using a rotary evaporator and dried at 60 °C in a vacuum oven. A yellow liquid with high viscosity was obtained (M_w = 2420 kg mol^{-1}).

Preparation and DIW of RDX-MOF ink

As shown in Fig. 2a, the GAP binder was completely dissolved in chloroform, and the explosive RDX and additive MIL-101(Cr) were added to the solution in the desired set ratio. The solution was then mixed uniformly using a stirrer and sonicated.

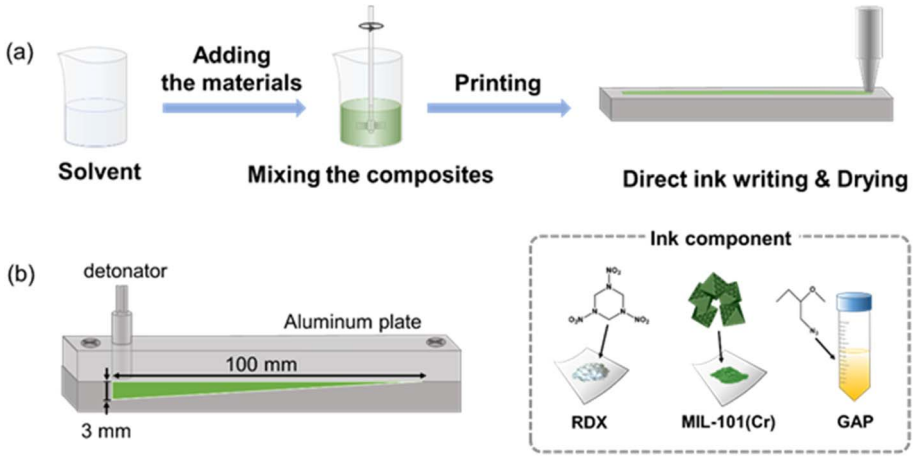

Fig. 2 Schemes depicting (a) the preparation process of RDX composites pattern using the DIW method and (b) the aluminium substrates with grooves.

The solvent was evaporated at 50 °C in a hot plate to form a slurry. The slurry was printed on the aluminium plate.

Evaluation of the critical diameter for detonation

A detonation test was conducted to evaluate the critical diameter after detonation using an exploding bridge wire (EBW) detonator (detonator Rp87, blaster FS-17). An aluminium substrate with grooves measuring 1 mm in width and 100 mm in length, was employed to assess the critical diameter for detonation (Fig. 2b). The depth of the grooves tapered from 3 mm to 0 mm, with a slope of 1.72° between the bottom and top of the furrow, facilitating the determination of the critical diameter after detonation. The critical diameter after detonation was calculated using the following eqn (1).

$$D = L \tan 1.72 \quad (1)$$

where D [mm] represents the critical diameter (depth) and L denotes the length at which detonation occurred.

The RDX-based pattern was printed on a tapered groove of the aluminium substrate using DIW and allowed to dry completely. After covering the substrate with the same material, the detonator was positioned in contact with the RDX pattern (Fig. 2b). A detonation test was subsequently performed to assess the critical diameter.

Characterization

Nitrogen adsorption measurements were conducted on a Micromeritics ASAP 2050 analyser at −196.15 °C after samples were preheated at 150 °C under vacuum for 12 h. The Brunauer–Emmett–Teller (BET) method was used to determine specific surface area and pore size distribution. Powder X-ray diffraction (PXRD) patterns were collected using a Rigaku D/Max2200 V X-ray diffractometer, with a scanning voltage of 40 kV and current of 40 mA. The samples were scanned at a speed of 3° min^{-1} over a 2θ range of 2–40°. Scanning electron microscopy (SEM) were employed to examine the morphology of the MOFs Philips XL30S FEG (10 kV) microscope. Attenuated total reflection Fourier transform infrared (ATR-FTIR) spectra were obtained using Nicolet 6700 (Thermo Scientific, MA, USA) to characterize the samples containing explosives. Spectra were recorded in the range 4000–400 cm^{-1}. ^1H NMR was performed to confirm the azidation of PECH to GAP using Brucker DPX-500FT NMR spectroscopy (Bruker, MA, USA). The molecular weight of GAP was measured by e2695 (Waters Co., MA, USA). The rheological properties of RDX based inks were investigated using a viscolite 700 portable viscometer after immersing the probe in the 50 mL of RDX ink with stirring. The thermal analysis of GAP was carried out using thermogravimetric analysis (TGA-N1000, Scinco M&T, Korea) at a ramping rate of 10 °C min^{-1} up to 500 °C under a constant flow of nitrogen (30 mL min^{-1}). The MIL-101(Cr) ratio in the RDX composites was investigated using an inductively coupled plasma-atomic emission spectrometer (ICP-AES, Thermo Fisher Scientific iCAP 6500 Duo) under the Ar purge. For ICP analysis, the solid-phase composites were prepared by completely removing the solvent from the RDX ink. The solid composite containing MOFs, RDX, and polymer binder, were completely dissolved in the solvent during the pre-treatment process using sulphuric acid and then analyzed.

Results and discussion

Characterization of MIL-101(Cr) and GAP

MIL-101(Cr) with regular nanopores (<4 nm) and a high pore volume was chosen as an additive for the RDX composites and was synthesised *via* a solvothermal reaction. MIL-101(Cr) was characterised by N_2 isotherms, pore size distribution, PXRD, IR spectroscopy, TGA and SEM (Fig. S1†). N_2 adsorption and desorption isotherms and pore size distribution (Fig. S1a and b†) showed a typical IV-type isotherm, indicating the mesoporous structure of MIL-101(Cr). The Brunauer–Emmett–Teller (BET) method estimated a specific surface area of approximately 2524 m^2 g^{-1} and a total pore volume of approximately 1.4 cm^3 g^{-1} at a relative pressure of $P/P_0 = 0.99$. PXRD patterns of MIL-101(Cr) closely matched the simulated pattern of MIL-101(Cr)

(Fig. S1c†). Sharp characteristic peaks below 10° confirmed that MIL-101(Cr) was highly crystalline. In the IR spectrum, the peaks at 1404 cm^{-1} indicated symmetric (O–C–O) vibrations, suggesting the presence of dicarboxylate, whereas the peaks at 1508 cm^{-1} represent stretching vibrations of (C=C) in the benzene ring (Fig. S1d†). MIL-101(Cr) shows thermal stability until 400 °C then decomposes with 60 wt% weight loss under N_2 atmosphere (Fig. S1e†). A uniform octahedral morphology with an average size of 600 nm was observed in the microscopic image (Fig. S1f†).

GAP was synthesised in two steps: the polymerisation and azidation of PECH (Fig. S3†). Peaks observed at 2094 cm^{-1} and 3500 cm^{-1} corresponded to the $-N_3$ stretching vibration and terminated OH groups, respectively (Fig. S3a†). The TGA curve showed a steep weight loss at 200 °C, similar to existing literature (Fig. S3c†). The ^{1}H-NMR data showed the main characteristic peak at 3.37 ppm corresponding to the methylene protons of the azidomethyl groups ($-CH_2N_3$), 3.52–3.72 ppm due to the methylene protons of the polyether main chain, and 3.95 ppm belonging to –OH (Fig. S3d†). The molecular weight of the resulting GAP was 2420 g mol^{-1} (number-average molecular weight, M_n), with a polydispersity index (PDI) of 1.5 (M_n/M_w).

RDX-MIL-101(Cr) ink

A previous study found that achieving high levels of RDX filling within the nanopores of MOFs exceeding 90% led to reduction in sensitivity to RDX. This was attributed to the decreased internal voids within RDX caused by its encapsulation within the nanoporous MOFs, as well as the rigid three-dimensional structure of the MOF. However, when RDX was simply mixed with MOFs without encapsulation, sensitivity increased significantly, leading to detonation at lower energy levels. Given the varying sensitivities of RDX upon the addition of MOF, MIL-101(Cr) was mixed with an RDX-based ink comprising GAP as a binder and chloroform as a solvent. Chloroform was chosen as the solvent as it effectively dissolved GAP without dissolving RDX. This helps prevent the explosive from entering the pores of the MOF, which could otherwise lead to a reduction in sensitivity. The compositions of the RDX-MOF inks are listed in Table 1. The samples with the viscosity of 2.3 cp to 4.0 cp were prepared according to the different proportions of MIL-101(Cr) (Table S1†). The viscosity was increased as more solid component was added to the solvent, chloroform with a viscosity of 0.5 cp. The measurements of RDX ink had the similar viscosity to the existing ink of high energy materials.[8] The samples were denoted as RDX/MOF(0), (0.5), (1), (1.5), and (2), respectively. As the amount of added MOF increased, the viscosity of the sample slightly increased.

Table 1 Formulations of energetic inks with different RDX/GAP/MIL-101(Cr)

Sample	GAP	RDX-E	MOF(Cr)
RDX/MOF(0)	0.11 g	0.99 g	
	10%	90%	
RDX/MOF(0.5)	0.11 g	0.9845 g	0.0055 g
	10%	89.5%	0.5%
RDX/MOF(1)	0.11 g	0.979 g	0.011 g
	10%	89%	1%
RDX/MOF(1.5)	0.11 g	0.9735 g	0.0165 g
	10%	88.5%	1.5%
RDX/MOF(2)	0.11 g	0.968 g	0.022 g
	10%	88%	2%

RDX/MOF composite

The resultant RDX-MOF composites exhibited a crystallinity similar to that of raw RDX (Fig. S4a†). The characteristic peaks of GAP were not easily discernible due to its amorphous structure (Fig. S4b†). IR spectra confirmed that the RDX/MOF composites displayed characteristic peaks of both RDX and GAP. However, given the limited amount of material used in preparing the RDX ink, highly crystalline MOFs with specific functional groups could not be identified in either the IR or XRD data. To quantitatively assess the MIL-101 (Cr) ratio, inductively coupled plasma atomic emission spectroscopy (ICP-AES) measurements were conducted and compared with theoretically calculated values (Fig. 3). The results indicated a proportional increase in Cr content with increase in MOFs content, with slight differences. Microscopic analysis was performed to investigate the morphology and dispersity of the RDX-MOF composite components (Fig. 3). Micron-sized RDX particles were well dispersed within the GAP matrix. In particular, nano-sized MOF particles were well-dispersed in the RDX/MOF(2) composite (Fig. 4b).

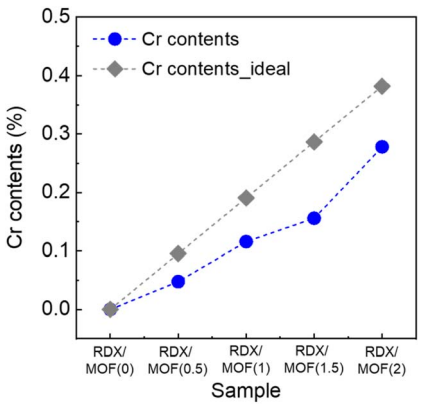

Fig. 3 Cr component in RDX ink obtained through ICP analysis and theoretically calculated value.

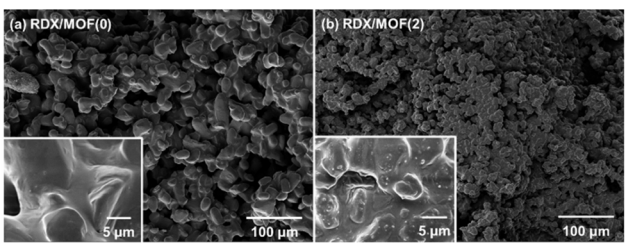

Fig. 4 FESEM images of RDX ink pattern of (a) RDX/GAP and (b) RDX/GAP/MOFs.

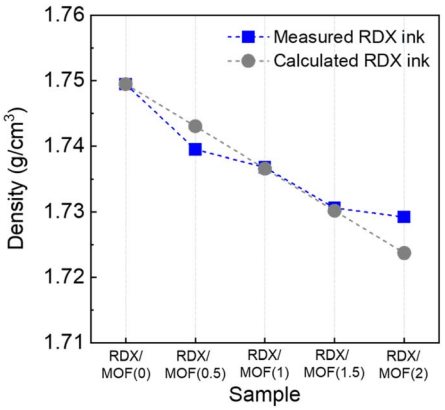

Fig. 5 Density of RDX ink measured by gas pycnometer.

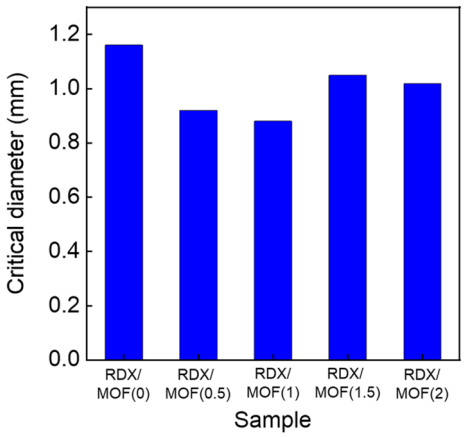

Fig. 7 Results of detonation test of RDX/MOF composites.

The localisation of RDX within or outside the pores of the MOFs significantly influences their sensitivity. To ascertain whether RDX was present inside or outside the pores, the densities of the RDX composite without MOFs and the RDX/MOF composites were measured using a gas pycnometer (Fig. 5). The theoretical densities were calculated assuming that RDX existed outside the pores of the MOF. The measured density values of the RDX/MOF composites closely matched the theoretical values, suggesting that RDX predominantly resides outside the pores rather than being encapsulated within them.

Critical diameter for detonation of RDX/MOF composites

The critical diameter of an explosive represents the smallest diameter that can sustain detonation to propagate and is a fundamental parameter for characterising explosives. The RDX/MOF ink was deposited on an aluminium substrate with a wedge-shaped groove using DIW. The groove's width was fixed at 1 mm, and its length was 100 mm, while the depth decreased gradually from 3 mm to 0 mm with a specific slope of 1.72° (Fig. 2b). After detonating the prepared samples, traces of explosions were observed on the plate (Fig. 6b). The length of the detonated trace varied depending on the MOF content in the ink. Component 3, containing 1 wt% Cr-based MOFs, resulted in the longest explosion trace because the designed nanopores efficiently transfer the heat generated during detonation (Fig. 7). However, with an increased MOFs concentration of 1.5 wt%, the presence of more MOFs served as combustible materials, absorbing the heat generated from explosives in the ink. Therefore, a long trace of the explosion was not observed.

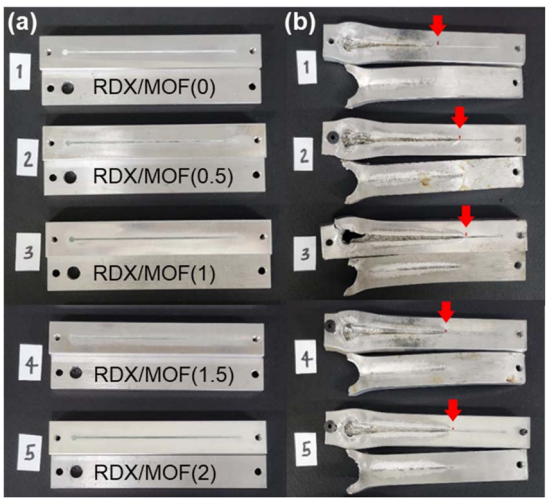

Fig. 6 Images of plate patterned with RDX/MOF ink (a) before and (b) after detonation.

Conclusions

The progression and integration of weapons systems have emphasized the need for explosive systems capable of operating in diverse environments. With the emergence of nanotechnology, numerous studies have reported the incorporation of novel materials into explosive formulations to optimise their performance. In this study, highly porous materials were introduced into explosive inks. The use of MIL-101(Cr) MOFs in RDX-based ink successfully created artificial hotspots, enabling detonation at low critical diameters. This innovation has the potential to significantly impact the development of compact and integrated weapon systems.

Data availability

All relevant data are within the manuscript and its additional files. The data are available from the corresponding author on reasonable request.

Author contributions

Eun-Young Kim – data curation, investigate, methodology, writing-original draft, visualization. Seong han Kim – investigate, methodology. Mingu Han – investigate, methodology. Su-Young Moon – conceptualization, supervision, writing-review & editing, funding acquisition.

Conflicts of interest

There are no conflicts to declare.

Acknowledgements

This work was supported by the Ministry of National Defense (MND) through the Defense Acquisition Program Administration (DAPA) (Grant No. 911555-911240001) and by the Korea Planning & Evaluation Institute of Industrial Technology (KEIT) and the Ministry of Trade, Industry & Energy (MOTIE) of the Republic of Korea (RS-2023-00267510).

Notes and references

1 M. P. Kroonblawd and L. E. Fried, *Phys. Rev. Lett.*, 2020, **124**, 206002.
2 W. Pang, C. Deng, H. Li, L. T. DeLuca, D. Ouyang, H. Xu and X. Fan, *Nanomaterials*, 2021, **12**, 133.
3 J. Xing, H. Zhang, L. Bai, G. Zhu, Q. Yu, B. Huang, Y. Liu, W. Wang, S. Li and Y. Liu, *Langmuir*, 2023, **39**, 3391–3399.
4 S. Manzoor, X. Yin and J.-G. Zhang, *Def. Technol.*, 2021, **17**, 1995–2010.
5 V. K. Balakrishnan, A. Halasz and J. Hawari, *Environ. Sci. Technol.*, 2003, **37**, 1838–1843.
6 H. Nan, Y. Zhu, G. Niu, X. Wang, P. Sun, F. Jiang and Y. Bu, *Crystals*, 2022, **13**, 35.
7 J. R. Verkouteren, *J. Forensic Sci.*, 2007, **52**, 335–340.
8 A. I. Brilian, V. Soum, S. Park, S. Lee, J. Kim, K. Kwon, O.-S. Kwon and K. Shin, *Micromachines*, 2021, **12**, 105.
9 W. Yang, R. Hu, L. Zheng, G. Yan and W. Yan, *Mater. Des.*, 2020, **192**, 108761.
10 K. C. To, S. Ben-Jaber and I. P. Parkin, *ACS Nano*, 2020, **14**, 10804–10833.
11 F. Yi, G. Gillen, J. Lawrence, T. P. Forbes, M. Staymates and D. A. LaVan, *Thermochim. Acta*, 2020, **685**, 178510.
12 J.-c. Zhang, K. He, D.-w. Zhang, J.-d. Dong, B. Li, Y.-j. Liu, G.-l. Gao and Z.-x. Jiang, *Energ. Mater. Front.*, 2022, **3**, 97–108.
13 O. Kudryashova, M. Lerner, A. Vorozhtsov, S. Sokolov and V. Promakhov, *Materials*, 2021, **14**, 7394.
14 M. Anniyappan, M. B. Talawar, R. K. Sinha and K. P. Murthy, *Combust., Explos. Shock Waves*, 2020, **56**, 495–519.
15 J. J. Pietron and P. B. Mirkarimi, *Propellants, Explos., Pyrotech.*, 2022, **47**, e202100379.
16 M. S. Eroglu and M. S. Bostan, *Org. Commun.*, 2017, **10**, 135–143.
17 T. Jarosz, A. Stolarczyk, A. Wawrzkiewicz-Jalowiecka, K. Pawlus and K. Miszczyszyn, *Molecules*, 2019, **24**, 4475.
18 H. J. Desai, D. O. Acheampong, R. Hudson, R. Lacey, C. Stanley, H. Turner, H. Whitmore, S. Torry, P. Golding and H. Erothu, *J. Energ. Mater.*, 2017, **35**, 109–124.
19 S. K. Shee, T. Reddy, S. Banerjee and A. K. Sikder, *J. Polym. Mater.*, 2015, **32**, 461.
20 M. M. Vala, Y. Bayat and M. Bayat, *Def. Sci. J.*, 2020, **70**, 461–468.
21 Y. Bayat, F. Jozi and T. Khanlari, *J. Energ. Mater.*, 2022, **40**, 153–169.
22 S. K. Reshmi, K. Vijayalakshmi, D. Thomas, E. Arunan and C. Reghunadhan Nair, *Propellants, Explos., Pyrotech.*, 2013, **38**, 525–532.
23 A. K. Hussein, A. Elbeih and S. Zeman, *RSC Adv.*, 2018, **8**, 17272–17278.
24 X. Zhou, Y. Mao, D. Zheng, L. Zhong, R. Wang, B. Gao and D. Wang, *J. Mater. Sci.*, 2021, **56**, 9171–9182.
25 M. N. Makhov, M. F. Gogulya, A. Y. Dolgoborodov, M. A. Brazhnikov, V. I. Arkhipov and V. I. Pepekin, *Combust., Explos. Shock Waves*, 2004, **40**, 458–466.
26 X. Mao, L. Jiang, C. Zhu and X. Wang, *Adv. Mater. Sci. Eng.*, 2018, **2018**, 1–8.
27 F. Xiao, W. Gao, J. Li and R. Yang, *Combust., Explos. Shock Waves*, 2020, **56**, 576–584.
28 Q. Li, C. An, X. Han, C. Xu, C. Song, B. Ye, B. Wu and J. Wang, *Propellants, Explos., Pyrotech.*, 2018, **43**, 533–537.